AUTHOR QUERIES

1. NO QUERIES

Genetic networks in Parkinson's and Alzheimer's disease

Jack Kelly[1], Rana Moyeed[2], Camille Carroll[1], Shouqing Luo[1], Xinzhong Li[3]

[1]Faculty of Health: Medicine, Dentistry and Human Sciences, Plymouth University, Plymouth PL6 8BU, UK
[2]Faculty of Science and Engineering, Plymouth University, Plymouth PL6 8BU, UK
[3]School of Science, Engineering and Design, Teesside University, Middlesbrough TS1 3BX, UK

Correspondence to: Xinzhong Li; **email:** X.Li@tees.ac.uk

ABSTRACT

Parkinson's disease (PD) and Alzheimer's disease (AD) are the most common neurodegenerative diseases and there is increasing evidence that they share common physiological and pathological links. Here we have conducted the largest network analysis of PD and AD based on their gene expressions in blood to date. We identified modules that were not preserved between disease and healthy control (HC) networks, and important hub genes and transcription factors (TFs) in these modules. We highlighted that the PD module not preserved in HCs was associated with insulin resistance, and *HDAC6* was identified as a hub gene in this module which may have the role of influencing tau phosphorylation and autophagic flux in neurodegenerative disease. The AD module associated with regulation of lipolysis in adipocytes and neuroactive ligand-receptor interaction was not preserved in healthy and mild cognitive impairment networks and the key hubs *TRPC5* and *BRAP* identified as potential targets for therapeutic treatments of AD. Our study demonstrated that PD and AD share common disrupted genetics and identified novel pathways, hub genes and TFs that may be new areas for mechanistic study and important targets in both diseases.

INTRODUCTION

Alzheimer's disease (AD) is the most common neurodegenerative disease (ND) and dementia, accounting for 60-80% of dementia cases. AD is characterized pathologically by accumulation of extracellular amyloid-β1 (Aβ) and deposits of intracellular tau neurofibrillary tangles [1]. In the US, the number of people living with AD is projected to increase from 5.5 million in 2018 to 13.8 million by 2050 [2]. Gradual progressive memory loss is the most common clinical symptom of AD, which eventually affects other cognitive functions such as communication and movement. There are currently many promising advances in the understanding of AD, including discovery of novel biomarkers [3, 4] and analysis of underlying biological mechanisms [5].

Parkinson's disease (PD) is the second most prevalent ND affecting approximately 145,000 people in the UK [6], and PD patient numbers are predicted to increase by 87.6% between 2015 and 2065 [6]. In the US, the number of PD cases are predicted to increase from 680,000 to 1,238,000 by 2030 [7]. The accumulation of α-synuclein in neurons in the form of Lewy bodies is the main neuropathologic hallmark of PD [8]. Primarily, PD affects the motor systems of the central nervous system (CNS) as a result of the death of dopamine generating cells in the midbrain substantia nigra (SN) [8].

There is growing evidence that AD and PD share many common characteristics [9]. Around 80% of PD patients will develop dementia, with an average time of onset 10 years from PD diagnosis [10]. We have recently shown that PD and AD share significant common differentially expressed genes (DEGs), disturbed pathways including the sirtuin signaling pathway, and identified *REST* as an important upstream regulator in both diseases [11]. AD and PD are both age-related diseases that have hallmarks of protein aggregation. In fact over 60% of AD cases are accompanied by the formation of Lewy bodies and α-synuclein is found as a non-amyloid component within AD amyloid plaques [12]. In addition, there are certain

genetic variants that increase the risk of both AD and PD, for example the strong risk factor for AD, APOE4, has been shown to be related to cognitive decline in PD [13].

Gene co-expression relationships contain a wealth of information that univariate methods like differential expression analysis cannot detect [14]. Weighted gene co-expression network analysis (WGCNA) is a popular tool used in systems biology to construct co-expression gene networks which can detect gene modules as well as identify key genes and hubs within these modules [15]. WGCNA has been used to find strong evidence for mitochondrial dysfunction and chronic low grade innate immune response in AD [16]. In addition, Chatterjee et al. [17] identified 11 hub genes by using WGCNA in frontal cortex and SN brain samples of PD patients.

To date there have been no studies investigating PD and AD using gene expression network simultaneously to reveal potential shared biological process and pathology. In this study we analyzed gene co-expression networks based on PD and AD blood microarray data and identified common genetic networks between both diseases. See our analysis workflow illustrated in Figure 1. Compared to brain tissues, blood tissue is easier to access from patients with ND, and publicly available AD and PD blood datasets have a large enough sample size to construct reliable and robust networks. Our network analysis expands on standard WGCNA and hub detection approach which can robustly find key processes and genes that are associated with both PD and AD.

RESULTS

Gene co-expression network construction

After quality control, we obtained 19176 genes in the PD dataset which included 204 PD and 230 healthy control (HC) samples, meanwhile 13661 genes were
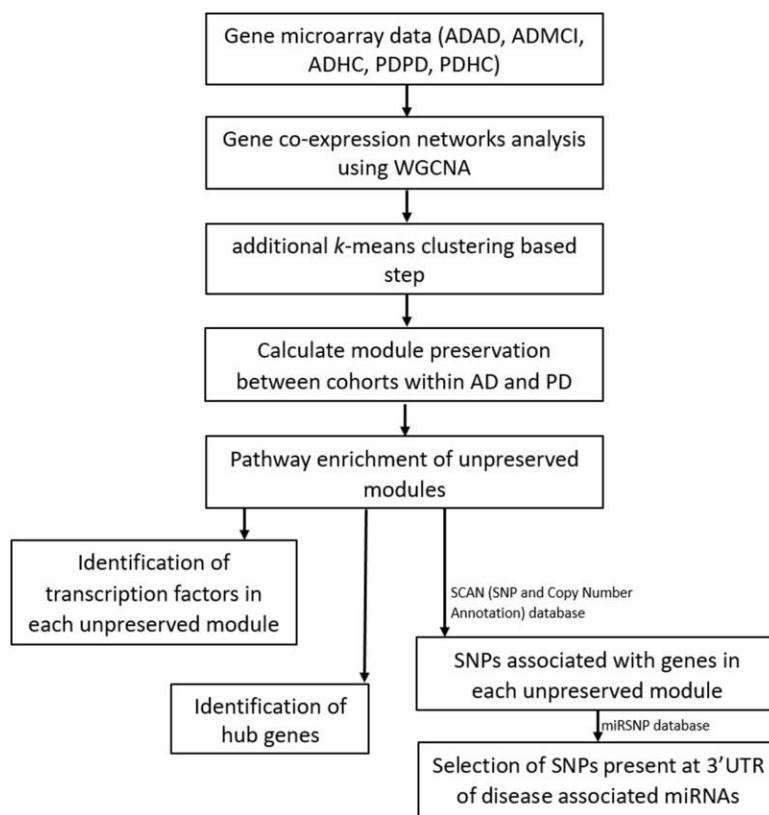

Figure 1. Workflow of our analysis. Filtered and normalized microarray data were separated into five datasets: AD disease (ADAD), healthy control (ADHC) and MCI (ADMCI) data from the AD dataset, and the PD disease (PDPD) and healthy control (PDHC) data from the PD dataset. On each dataset gene co-expression networks analysis was performed using the WGCNA R package [15]. An additional *k*-means correction step to reduce number of misplaced genes [70] was then performed and module preservation between cohorts within AD and PD was found using NetRep (v.1.2.1) [18]. The pathways associated with non-preserved modules were then found using the Enrichr web tool [19,20] and hub genes and transcription factors in these non-preserved modules identified. The SCAN (single nucleotide polymorphism (SNP) and Copy number ANnotation) database) database [25] was used to find SNPs associated with the genes in each non-preserved module and these SNPs used to search the MiRSNP database to find the SNPs at 3' UTR of disease associated miRNAs.

obtained in the AD dataset which included 245 AD, 142 mild cognitive impairment (MCI) and 182 HC samples. We applied WGCNA [15] to build our networks and selected the soft threshold power to define the adjacency matrix of each dataset based on approximate scale-free topology R^2 of 0.85 (Figure 2). In this method, highly correlated nodes are placed into a single module or cluster which are thought to be regulated by similar transcription factors (TFs) and represent certain biological processes. These networks were constructed for the AD disease (ADAD), healthy control (ADHC) and MCI (ADMCI) data from the AD dataset, and the PD disease (PDPD) and healthy control (PDHC) data from the PD dataset separately. We discovered 27, 54,

29, 32 and 58 modules in PDPD, PDHC, ADAD, ADMCI, ADHC networks respectively.

PD blood and brain DEG overlap

We identified 360 DEGs in the PD blood dataset (nominal Pvalue < 0.01, see Supplementary Table 2) and compared these DEGs to the DEGs identified in our recent meta-analysis study about PD in substantia nigra region [11]. An overlap of 21 genes were found including *LRRN3*, *BASP1* and *TPM3*. However, a Fisher Exact test was not significant for the overlap showing that this was likely by chance (OR = 1.08, 95% CI 0.65~1.72, Pvalue = 0.72, Fisher Exact test).
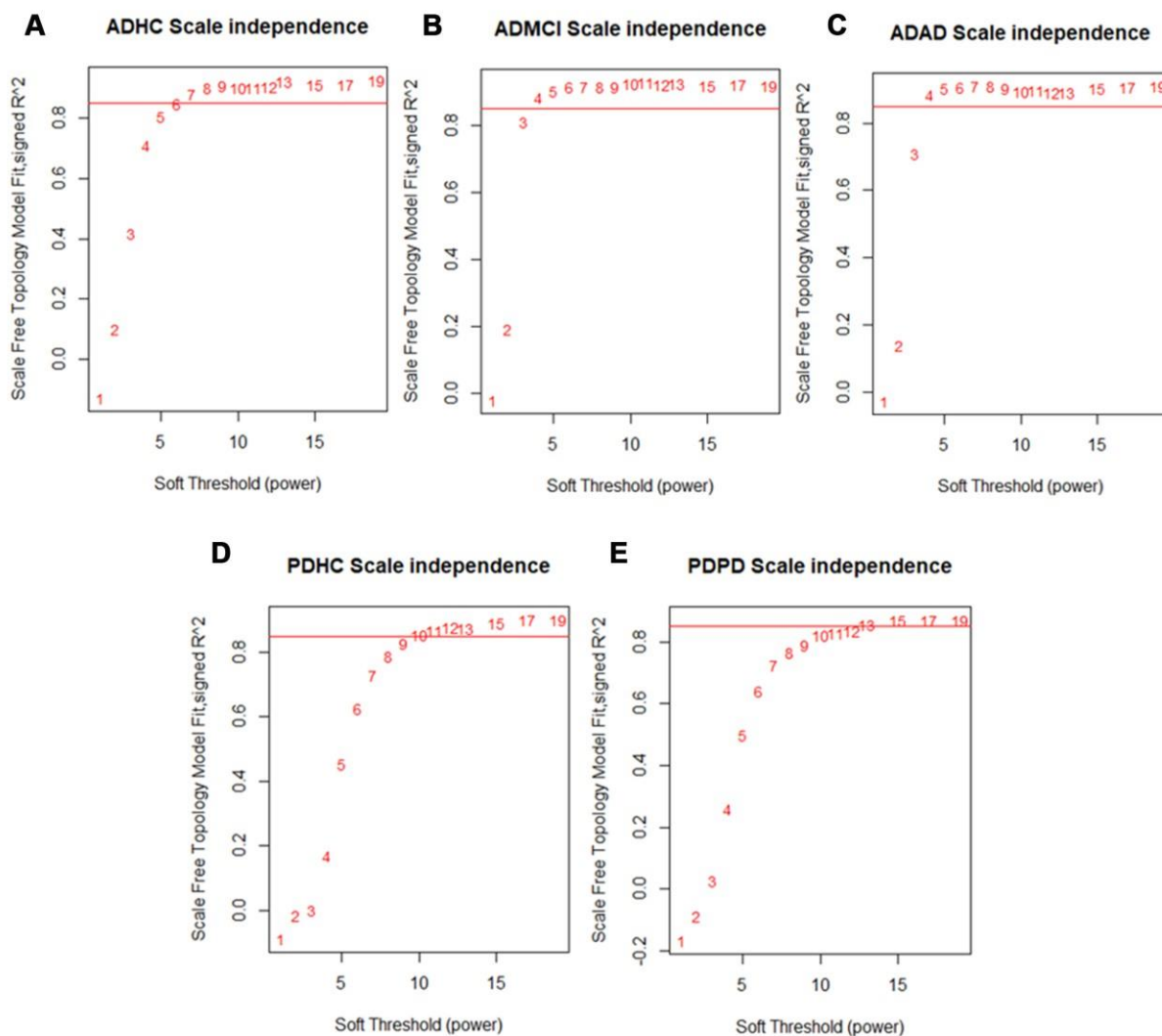
Figure 2. Scale free network topology (signed R²) for different soft-thresholding powers of data. A soft thresholding power that achieved a scale-free topology of R² of 0.85 was chosen to define approximate scale-free topology. We found that the (**A**) ADHC data achieved approximate scale-free topology at a soft thresholding power of 6 and the (**B**) ADMCI and (**C**) ADAD data at a soft thresholding power of 4. The (**D**) PDHC data reached approximate scale-free topology at a soft thresholding power of 10 and (**E**) PDPD data at a soft thresholding power of 13.

Identification of non-preserved modules

In our network analysis, if the relationships and correlation structure between nodes composing each module were not replicated, then they were considered non-preserved. In the case of healthy and disease networks, non-preserved modules suggested the expression pattern and regulation of the genes in these modules vary between disease and healthy conditions. On the other hand, modules preserved between disease and healthy networks represented processes that are not affected by disease status. Here we focused on non-preserved modules which may help to reveal the disease mechanism. The R package NetRep (v1.2.1) was used to identify these non-preserved modules [18].

Table 1 shows the non-preserved modules between PDHC and PDPD networks and the biological processes associated with these modules. Three of the 54 modules in the PDPD network were not preserved in PDHC network, and one of those 27 PDHC modules was not preserved in the PDPD network. The Gene Ontology (GO) and Kyoto Encyclopedia of Genes and Genomes (KEGG) terms that were significantly enriched within non-preserved modules (Pvalue < 0.01) were found using the Enrichr web tool [19, 20]. The PDPD salmon module was found to be associated with insulin signaling (KEGG pathway, Pvalue = 0.0030, 7/108 overlap). The PDPD darkseagreen4 module was found to be associated with antigen processing and presentation (KEGG pathway, Pvalue = 5.38E-16, overlap = 14/77) and natural killer cell mediated cytotoxicity (KEGG pathway, Pvalue = 2.94E-15, overlap = 10/41).

Table 2 shows the non-preserved modules between the ADHC, ADMCI and ADAD networks. Of the 29 ADAD modules, one was not preserved in both ADHC and ADMCI networks. In addition, one of the 32 ADMCI modules was not preserved in ADAD and ADHC networks. Moreover, three of the 58 ADHC modules were not preserved in both ADAD and ADMCI networks and one non-preserved in ADMCI networks. The ADAD blue module was not preserved in ADHC and ADMCI networks and was associated with regulation of lipolysis in adipocytes (KEGG pathway, Pvalue = 6.24E-4, overlap = 10/55) and neuroactive ligand-receptor interaction (KEGG pathway, Pvalue = 0.005070, overlap = 30/338). The ADHC darkolivegreen module was associated with sensory perception (GO biological process, Pvalue = 1.83E-4, overlap = 8/55).

Identifying hub genes

Hubs are genes that are highly interconnected or important within a module and likely have functional

significance [21]. Hubs have a role in maintaining the structure of the gene network of the module and the biological processes associated with the module. In our study, hub genes were identified using five approaches: Betweenness centrality (BC), PageRank, module membership (MM), closeness centrality and Kleinberg's centrality. Any gene with a Pvalue < 0.01 in any hub detection method was considered as a significant hub gene. Using multiple methods for identifying hubs allowed for hub identification that may otherwise have been missed by use of just one method. To demonstrate hub score distribution, Supplementary Figure 2A shows an example of betweenness hub score distribution across all genes in the PDPD darkseagreen4 module which was non-preserved in PDHC network and the (Supplementary Figure 2B) distribution of the significant *GINS2* (Pvalue = 0.005) BC scores across the 1000 iterations of the hub permutation test.

We identified 34 hubs in modules not preserved between the PDPD and PDHC networks (Supplementary Table 3) and 92 hubs in the non-preserved modules between ADAD, ADMCI and ADHC networks (Supplementary Table 4). It was expected that larger modules may have more hubs than smaller ones, for example the PDHC purple module contained 606 genes, of which 17 were found to be hubs (e.g. *FAM110C*, *PAK4*, *NEB*), and the smaller salmon PDPD module contained 351 genes, of which only 10 were hubs (e.g. *HDAC6*, *TYSND1*). The PD salmon module was associated with insulin resistance and was not preserved in PDHC network shown in Figure 3A, where hub genes are highlighted. Interestingly, it includes *HDAC6* which has been shown to influence tau phosphorylation and autophagic flux in AD [22]. The blue AD module which was associated with regulation of lipolysis in adipocytes and neuroactive ligand-receptor interaction and was not preserved in ADMCI and ADHC networks (Figure 3B) which included *TRPC5* and *BRAP* as hub genes. Networks were visualized in Gephi [23].

Identifying transcription factors (TFs)

Genes that are clustered together by WGNCA likely are regulated in a similar way, thus we intended to identify which TFs potentially regulate the gene expression of each module. The TFs that potentially regulate each non-preserved module (Pvalue <0.01) were identified by using Encyclopedia of DNA Elements (ENCODE) and chromatin immunoprecipitation (ChIP) Enrichment Analysis (ChEA) consensus TFs from ChIP-X by using the Enrichr web tool [19,20]. We found a total of four TFs that regulated at least one of the three PDPD modules, including *FOXM1* which regulated 6 genes in the salmon modules (Pvalue = 0.0066) and 9 in the

Table 1. List of non-preserved modules found between PD and healthy controls (HC).

Module colour	Pvalue of NetRep	Processes associated with module found using Enrichr	No. genes in module
PD modules not preserved in HC			
Darkseagreen4	9.99E-5	Antigen processing and presentation, Natural killer cell mediated cytotoxicity, cellular defense response, regulation of immune response	150
Navajowhite2	9.99E-5	cellular response to misfolded protein	150
Salmon	9.99E-5	Insulin resistance, regulation of protein homooligomerization	351
HC modules not preserved in PD			
Purple	9.99E-5	Antigen processing and presentation, VEGF signaling pathway, regulation of intracellular transport	606

Table 2. List of non-preserved modules found between AD, MCI and healthy controls (HC).

Module colour	Pvalue of NetRep	Processes associated with module found using Enrichr	No. genes in module
AD modules not preserved in HC			
Blue	9.99E-5	Regulation of lipolysis in adipocytes, Neuroactive ligand-receptor interaction, detection of chemical stimulus involved in sensory perception of smell, extracellular matrix organization	1076
AD modules not preserved in MCI			
Blue	9.99E-5	Regulation of lipolysis in adipocytes, Neuroactive ligand-receptor interaction, detection of chemical stimulus involved in sensory perception of smell, extracellular matrix organization	1076
MCI modules not preserved in AD			
Sienna3	8.59E-3	Regulation of lipolysis in adipocytes, axonal fasciculation, hippo signaling	770
MCI modules not preserved in HC			
Sienna3	9.99E-5	Regulation of lipolysis in adipocytes, axonal fasciculation, hippo signaling	770
HC modules not preserved in AD			
Darkolivegreen	9.99E-5	sensory perception, regulation of potassium ion transmembrane transport	584
Darkorange2	0.011	Peroxisome, amide transport	248
Skyblue	0.015	establishment of epithelial cell polarity	187
HC modules not preserved in MCI			
Darkolivegreen	9.99E-5	sensory perception, regulation of potassium ion transmembrane transport	584
Red	9.99E-5	Regulation of lipolysis in adipocytes, bicellular tight junction assembly	704
Darkorange2	2.99E-4	Peroxisome, amide transport	248
Skyblue	0.022	establishment of epithelial cell polarity	187

darkseagreen4 module (Pvalue = 4.00E-08). Within one PDHC module, there were a total of six TFs, including *CREB1* which regulated 64 genes in the purple module (Pvalue = 0.001402). Supplementary Table 5 shows the significant TFs found in modules that were not preserved between PD and HC networks.

We found two TFs (*SUZ12*, *EZH2*) regulating non-preserved ADAD modules, and one TF (*SUZ12*) regulating 115 genes in the ADMCI sienna3 module (Pvalue = 8.24E-10). We also identified 18 TFs that regulated at least one of four non-preserved ADHC modules. This included *REST* which regulated 20 genes

in the darkolivegreen (Pvalue = 0.0092) and *SUZ12* which regulated 68 genes in the darkolivegreen (Pvalue = 0.0039) and 107 genes in the red module (Pvalue = 1.21E-09). In addition, *CREB1* regulated 29 genes in the ADHC darkorange2 module (Pvalue = 0.007005). Supplementary Table 6 shows the same for modules that were not preserved between ADAD, ADMCI and ADHC.

Single nucleotide polymorphism (SNP) analysis of significant WGCNA modules

As non-preserved modules contain genes which play a role in processes that were associated with AD or PD, they may have been more likely to contain disease associated variants than preserved modules. We searched each non-preserved PD module for known Genome Wide Association Studies (GWAS) genes associated with PD [24]. There are 69 known GWAS genes, of which four (*TMEM163, TLR9, ITIH4, TUBG2*) were in the salmon module and two (*TMEM175, STAB1*) were in the navajowhite2 module. We observed a significant enrichment of GWAS genes within modules that were not preserved compared to preserved networks (OR = 2.96, 95% CI 1.04~6.88, Pvalue = 0.02, Fisher Exact test). Furthermore, the non-preserved PDHC purple network contained five GWAS gene (*KAT8, BIN3, TLR9, ITIH4, TUBG2*), however the non-preserved HC modules were not more likely to contain GWAS genes (OR = 2.61, 95% CI 0.08~6.47,

Pvalue = 0.052, Fisher Exact test). We did the same analysis for the non-preserved AD modules, however, no AD associated GWAS genes were found within any non-preserved modules.

In addition to searching for known GWAS genes in non-preserved modules, we used the SCAN (SNP and Copy number ANnotation) database (http://www. scandb.org/) [25] to identify SNPs corresponding to the genes in each non-preserved module. These SNPs were used to search the MirSNP [26] database to identify SNPs associated with known PD or AD microRNAs (miRNAs) dependent on the dataset of the module. We identified 29 SNPs associated with 9 PD related miRNAs across all non-preserved modules in the PD dataset (Supplementary Table 7), and 27 SNPs associated with 8 AD related miRNAs across all non-preserved modules in the AD dataset (Supplementary Table 8).

Comparison of AD and PD results

There is increasing evidence that PD and AD share several common characteristics [9], thus we investigated the shared processes associated with non-preserved modules in both the AD and PD dataset to see which were important in both diseases. The biological processes found to be associated with significant modules in AD and PD were compared to see which were important in both diseases. Unfortunately, we did
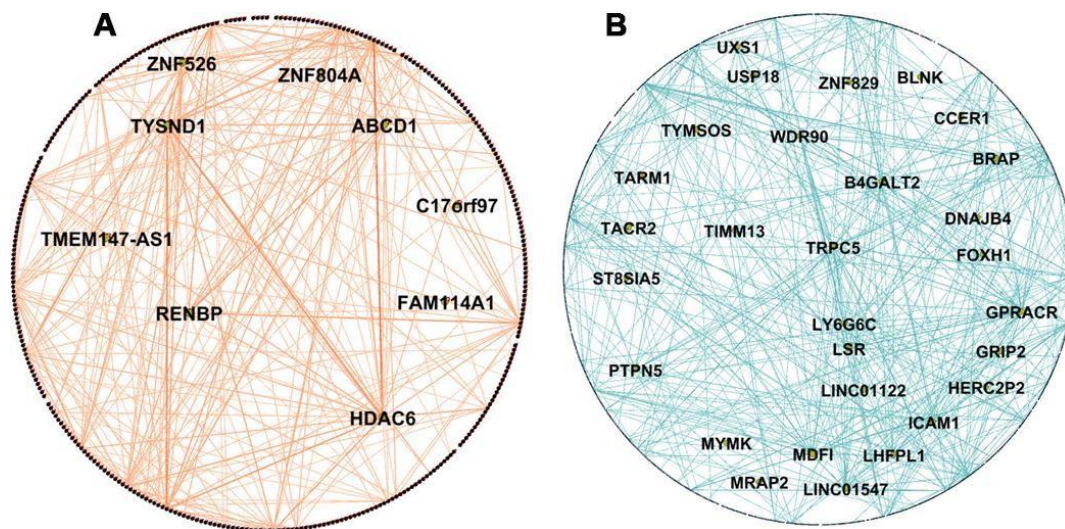
Figure 3. Network visualization of PD and AD modules. (**A**) Visualization of WGCNA network connections of the PDPD salmon network module found to be associated with insulin resistance and not preserved in the PDHC network. It shows network connections whose adjacency is above 0.2, including all 351 nodes and 595 of 61776 edges. (**B**) Visualization of WGCNA network connections of the ADAD blue module found to be associated with regulation of lipolysis in adipocytes and neuroactive ligand-receptor interaction and not preserved in ADHC and ADMCI networks. It shows network connections whose adjacency is above 0.55, including all 1076 nodes and 1458 of 1157776 edges. Hub genes are in the center of the network and are labelled with names. Networks visualized in Gephi [23].

not find any significant modules that were common between these two. However, we identifed some similarities between AD and PD. The PDHC purple module and the ADHC darkorange2 module had four significant TFs which regulate both modules (*SIX5, CREB1, NFYB, PBX3*). Of those 29 PD SNPs and 27 AD SNPs we have identified, 12 were common between the two. The genes associated with these SNPs were: *EPB41L5, CYP26B1, IQCB1, DCP1A, CLGN, TDRD6, PSORS1C1, PARP12, WISP1, PIK3C2A, CLMN, DHX33* which are highlighted in Supplementary Tables 7 and 8.

Data accession

The hub scores for each gene in PD modules not preserved in HC networks can be accessed and downloaded from https://jack-kelly.shinyapps.io/pdpd_hubs/. The same information for HC modules not preserved in PD networks can be found at https://jack-kelly.shinyapps.io/pdhc_hubs/.

The hub scores for each gene in the AD modules not preserved in HC or MCI networks can be found at https://jack-kelly.shinyapps.io/adad_hubs/. The same for MCI modules not preserved in HC or AD networks can be found at https://jack-kelly.shinyapps.io/admci_hubs/ and for HC modules not preserved in MCI or AD networks at https://jack-kelly.shinyapps.io/adhc_hubs/.

DISCUSSION

In this study, by using gene co-expression network analysis we identified many important biological processes and key genes in PD and AD blood samples, and the common results between them. To our knowledge this is the largest network analysis of AD and PD blood to date. We found insulin resistance to be associated with PD and *HDAC6* may play an important role in this process. We highlight the overlap in disease miRNA associated SNPs that are shared between PD and AD, suggesting similarities in genetic risk factors between the diseases. Our approach used blood data as the available blood datasets have a large enough sample size to construct robust and reliable networks and blood samples are easily accessible in neurodegenerative disease patients. We previously found that DEGs in AD blood were more likely to be DEGs in AD brain tissue [27]. However, in this study, we found that DEGs in blood were not more likely to be DEGs in brain tissue for PD, nevertheless it has been shown that changes in blood gene expression did reflect changes in PD [28].

The PD network module associated with insulin resistance is not preserved in HCs. Insulin resistance is increasingly being shown to be important in PD as a

potential therapeutic target [29] and has a high prevalence in non-diabetic PD patients [30], additionally insulin receptor signaling pathways are disturbed in PD [11]. Within this module we identified *HDAC6* as a hub gene which promotes the formation of inclusions from α-synuclein toxic oligomers [31]. *HDAC6* can promote insulin resistance by deacetylating phosphatase and tensin homolog (PTEN) in ovarian OVCAR-3 cells [32], and PTEN has in turn been shown to be involved in the pathophysiology of PD [33]. *HDAC6* has a role in influencing tau phosphorylation and autophagic flux in neurodegenerative disease [22]. In addition, insulin signaling promotes the DNA-binding activity of *FOXM1*, identified as a significant TF in the insulin resistance module, which regulates pathways to promote adaptive pancreatic β cell proliferation [34], but its role in ND is not clear.

The PD module associated with cellular response to misfolded proteins was also not preserved in HC networks. PD is characterized by accumulation of misfolded α-synuclein and a failure of the proteasome to degrade these and other large protein aggregates [35]. The hub gene *SNRNP70* has been shown to be differentially expressed in PD blood previously [36]. Additionally, *SNRNP70* encodes the small nuclear ribonucleoprotein snRNP70 which co-localizes with tau in AD [37], and as tau aggregation is shown in ~50% of PD cases snRNP70 may colocalize in PD cases [38]. We also identified *MIR142*, which encodes miRNA-142, as a hub. miRNA-142 has been identified as an important miRNA in PD, regulating GNAQ, TMTC2, BEND2, and KYNU [39].

The AD module associated with regulation of lipolysis in adipocytes and neuroactive ligand-receptor interaction was not preserved in both MCI and HC networks. Aβ, a key molecule in AD brain pathology, can induce lipolysis within human adipose tissue [40]. In addition, lipolysis is promoted by insulin resistance and in turn lipolysis generates ceramides further impairing insulin signaling, which is becoming increasingly more important in AD [41]. We identified *TRPC5* as a hub in this module, which along with other transient receptor potential canonical (TRPC) proteins assembles to form non-selective Ca2+-permeable channels. Another hub, *BRAP*, has a polymorphism associated with obesity and other metabolic traits, which can play a role in effecting insulin signaling and aging [42]. Interestingly, a module in the HC network that was not preserved in AD and MCI networks was also associated with regulation of lipolysis in adipocytes. This suggests that these processes are occurring in both healthy and AD conditions, however the enrichment pathways are different between the two. As no hubs are shared between the regulation of

lipolysis in adipocytes modules in healthy and AD networks they are likely regulated differently.

The module associated with sensory perception in the HC network was not preserved in AD and MCI networks. Sensory dysfunction may precede the cognitive symptoms of AD [43], particularly olfactory impairment [44]. *OR5AS1* was identified as a hub gene within the module which encodes a member of the olfactory receptor family and plays a role in triggering response to smells [45]. The TF *REST* was identified as a regulator of the module and has been shown to regulate olfactory systems [46]. We have identified *REST* to be an important upstream TF for DEGs identified in both AD and PD previously, and as an important potential therapeutic target [11]. Future work to validate our identified hubs and TFs in both AD and PD disease models would further elucidate their potential as targets for disease treatment.

Although we did not identify any common non-preserved modules in the AD and PD cohorts, there were other similarities shared in the results. Four TFs were shared between the PDHC purple and the ADHC darkorange2 module (*CREB1, NFYB, PBX3, SIX5*). These two modules were associated with different transport pathways in HCs which were not preserved in the disease networks, suggesting that the roles of these TFs are dysregulated in both AD and PD. In addition to this, we identified 12 SNPs that were shared between the 29 PD miRNAs associated SNPs and 27 AD miRNAs associated SNPs. This number of shared SNPs is highly significant, which suggests that there are potential risk factors that underlie both diseases.

Several studies have applied WGCNA in ND studies for gene expression and proteomics analysis. For example, Seyfried and colleagues studied proteomic data of cortical tissue of asymptomatic and symptomatic AD [47]. They found that there was a modest overlap between networks at RNA and protein level. If a larger dataset becomes available, expanding our methods to proteomic data could give further understanding into the mechanisms of AD and PD and enable the investigation into the link between genomics and proteomics. Chatterjee et al. [17] have performed network analysis of PD brain tissue, however they only performed WGCNA on DEGs found in the data, which built very limited networks that removed potentially important gene interactions and disease regulators and introduced a bias of modules and hubs towards these DEGs. In addition, they used tissue from multiple brain regions which would all be affected differently by the disease [48].

A limitation of this study is that, although it has been shown that AD blood DEGs are more likely to be

DEGs in the brain [27], our results suggest this is not the case for PD. Because of this, our results may not reflect major changes that take place in the brain. However, our network analysis approach emphasizes the interactions of genes which univariate methods like differential expression does not. Similarly to AD, there is disruption that happens in the blood brain barrier (BBB) of PD patients [49]. Hence, it is likely that changes that take place in the brain could be reflected in the blood and vice versa. Additionally, a lot of the biological processes and genes we found in our PD network has been implicated in the PD brain previously [11]. Tau and Aβ are hallmarks of both AD and PD in the brain and have potential as blood biomarkers in both diseases [50, 51], suggesting that changes in the brain are reflected in blood. Leukocytes have been shown to impact progression of neurodegenerative diseases. An interaction between brain and systemic inflammation has been implicated in PD progression by an association between leukocyte apoptosis and central dopamine neuron loss [55]. Increased mitochondrial respiratory activity in leukocytes has been shown in PD patients, potentially impacting progression of neurodegeneration [56] and elevated leukocytes in cerebrospinal fluid are significantly associated with shorter survival of patients [57]. Peripheral leukocytes have been discussed as potential biomarkers for AD previously [52], and gene expression changes in leukocytes have been shown to be closely associated with AD progression [53]. In AD animal models circulating leukocytes have been shown to cross a dysfunctional blood brain barrier and impact brain integrity [54].

Recently limbic-predominant age-related TDP-43 encephalopathy (LATE) has been reported to be under-recognized and often misdiagnosed as AD as they share common pathogenetic mechanisms and present similarly in patients [58]. There is the potential that patients in our AD cohort may have been misdiagnosed and actually have LATE, however as LATE is seen with increasing frequency over the age of 85, and less than 6% of our AD samples were over the age of 85 this likely had little effect on our results.

The greatest risk factor for both AD and PD is age. Adjusting AD data by age before WGCNA ensured any changes we found were reflective of disease state. The PD data, however, did not include samples' age information when we downloaded, thus the effect of age could not be removed technically. As a result of this, the PD results may have been biased towards changes as a result of aging if there was a significant difference in age between PD and HC cohorts. However, the samples were age matched in the original design which should reduce such biases [59].

From the PD dataset we removed patient samples with known PD mutations. Although the biological pathways underlying familial and sporadic forms of PD are likely to be shared, known PD mutations may impact pathways to disease or regulators of disease [60]. Removal of samples with known PD mutations prevented these mutations from having an impact on results, however had little impact on sample size due to the low number of samples with mutations. AD samples were not screened for known mutations, which could have had an impact on our results. For example, nearly 19% of the familial late onset AD population carry 2 APOE ε4 alleles which only occurs in about 1% of normal Caucasian controls [61]. This and other known mutations may impact the progression and regulators of AD, and knowing which samples had these mutations could have improved our findings.

In conclusion, our network analysis is the largest study using AD and PD blood data to date. We highlight the non-preserved module in PD associated with insulin resistance, and the hub *HDAC6* identified in this module. Our results reveal that a large proportion of disease miRNA associated SNPs are shared between PD and AD, suggesting similarities in genetic risk factors between the diseases. The hub genes that we have identified have the possibility to be further investigated as potential biomarkers for disease. These insights suggest several new areas for mechanistic studies in PD and AD research fields.

MATERIALS AND METHODS

Data preparation for PD and AD blood datasets

The publicly available peripheral venous whole blood dataset comprising 205 PD and 233 control samples was downloaded from the GEO (Gene Expression Omnibus) database (http://www.ncbi.nlm.nih.gov/geo/) with accession identifier GSE99039. This dataset is the largest of its type and has a sample size enough to run WGCNA and reliably find hub genes [62]. Samples with known PD mutation genes (*Parkin, DJ-1* and *PINK1, ATP13A2, LRRK2, SNCA*) were removed to reduce biases introduced by these genes (see discussion), and outlier samples were detected and removed based on box and density plots of probe intensities. This removed a total of one PD and three HC samples, leaving 204 PD and 230 HC samples. Data was then Robust Multiarray Average (RMA) normalized using the affy R package [63]. Samples missing gender information (35 samples) were assigned sex by using the massiR R package [64] which uses the information from microarray probes that represent genes in Y chromosome to perform k-medoids clustering to classify the samples into male and female

groups. We selected a probe-variation threshold of 4 by inspecting a probe-variation plot (Supplementary Figure 1) to select the Y chromosome probes to be used in the sex classification process.

The ComBat function in the sva R package [65] was used to control the effect of gender and running batch of the samples. After this, control probes and those without Entrez gene annotation were removed. For any genes that mapped to multiple probes, the probe with the highest median absolute deviation (MAD) was kept. MAD was used as, similarly to inter-quartile range, the probe with the highest MAD has the greatest variability and so likely has more information [66]. Finally, the bottom 5% probes by average expression values across all samples were removed.

For AD, the two independent peripheral venous whole blood datasets GSE63060 and GSE63061, from the AddNeuroMed Cohort [67], were used to construct the blood gene expression networks. As these two datasets were from the same cohort study and sample collection and analysis was carried out using the same methodologies, except using different biological samples and microarray platforms, they can be merged to produce a larger dataset that can improve the power of our study. The two normalized datasets (generated by different Illumina platforms) were merged using the inSilicoMerging R package [68], which removes the batch effects between these two, as we have done previously [27].

Patients of Western European and Caucasian ethnicity were extracted from the merged dataset leaving a total of 245 AD, 142 MCI and 182 HC to reduce any potential genetic impact that ethnicity may have on AD. The effect of the age and gender were controlled for using the ComBat function in the sva R package [65]. As with the PD data, control probes and those without Entrez gene annotation were removed and for any genes that mapped to multiple probes, the probe with the highest MAD was kept. Finally, the bottom 5% probes by average expression values across samples were removed. Information on number of samples, gender and age of samples is shown in Supplementary Table 1.

PD blood and brain DEG overlap

To see if there was a significant overlap between PD gene expression in blood and brain as has been shown previously in AD [27], our data was compared to DEGs previously identified in PD substantia nigra [11]. Using the normalized and filtered PD data, DEGs were identified by applying limma with gender and running batch adjusted. Slightly stringent nominal Pvalue <0.01

was used for significance as only one DEG could pass multiple testing (FDR corrected Pvalue <0.05).

Gene co-expression network construction

The R package WGCNA [15] was applied to perform gene co-expression network analysis as follows: A matrix of pairwise correlations between all pairs of genes across each sample group (e.g. case and control groups separately), was created and each raised to a soft-thresholding power to achieve a scale-free topology R^2 of 0.85. From this, a topological overlap matrix (TOM) was calculated, which takes correlation between genes expression as well as connections the genes share into consideration. This TOM was then converted to topological overlap dissimilarities to be used with hierarchical clustering. Then, a dynamic tree-cutting algorithm was used to determine initial module assignments of genes (cutreeHybrid, using default parameters except deepSplit of 3, minModuleSize of 10 and mergeCutHeight of 0.05) [69]. An additional *k*-means clustering step was applied to improve the results of the hierarchical clustering in WGCNA as proposed by Botía et al [70] which has been reported to be able to reduce the number of misplaced genes and improve the enrichment of GO pathway terms. All analysis was conducted in R3.5.2 [71].

Calculation of module preservation

In order to identify modules that are not preserved between conditions within datasets, we applied NetRep (v1.2.1) [18] which uses a permutation test procedure on seven module preservation statistics. We permuted 10,000 times. The "alternative" parameter is set to "less" to test whether each module preservation statistic is smaller than expected by chance in order to identify these non-preserved modules which are extremely different in the two networks. If all seven module preservation statistics had a Pvalue < 0.05 then that module was significantly non-preserved between conditions.

Pathway enrichment analysis

To identify the biological pathways that the modules represent we performed GO and KEGG pathway enrichment analysis (KEGG 2019) using the Enrichr web tool [19, 20]. Pathways and GO terms with a Pvalue < 0.05 were considered significant.

Hub gene identification

Generally, detecting hub genes in co-expression networks has been done using MM, which is the correlation of a gene to its eigengene (the first principle component calculated using the expression data of

genes in each module) [72]. BC of a gene is the number of shortest paths connecting all gene pairs that pass through that gene [73], and genes with high BC were considered as "high traffic".

Here we have expanded hub detection to include multiple other hub detection methods frequently used in network analysis. In addition to MM and BC, we used closeness centrality [74], Kleinberg's hub centrality score [75] and the PageRank algorithm [76] which would reduce the chance of missing any important hub genes that regulate the network that may be missed by applying individual methods. Genes with high closeness centrality scores have the shortest path to all other genes in the module and are placed to influence the entire network quickly [74]. PageRank emphasizes nodes that are connected to other nodes with high Pagerank scores [76]. Kleinberg's hub centrality score [75] is similar to the PageRank algorithm, however, the small differences between the two widens the net for identifying important hubs.

A novel hub detection permutation test was developed to obtain Pvalues for each hub detection store and determine if they are statistically significant. Briefly, the gene ID labels on the adjacency matrix were randomly re-labelled and hub score recalculated 1000 times to obtain a statistical distribution. The Pvalue was calculated by dividing the number of recalculated permutation hub scores that are higher than the observed hub score in the original network by the number of permutations. Genes were considered significant hubs if any hub scores had a Pvalue < 0.01. This was performed for all modules not preserved between PD and HCs in the PD dataset, and the modules not preserved between any of the AD, MCI and HCs networks in the AD dataset. BC, closeness centrality, PageRank and Kleinberg's hub centrality scores were calculated using the igraph R package with default settings without normalization [77]. The R code used for the novel hub detection test is available at http://dx.doi.org/10.5281/zenodo.3686007.

Identifying transcription factors

To identify TFs that potentially regulate each module, we used ENCODE and ChEA Consensus TFs from ChIP-X found using the Enrichr web tool [19, 20]. TFs with a Pvalue < 0.01 were considered significant. If a TF was found significant in both ENCODE and ChEA then the lower Pvalue was assigned to the TF.

SNP and microRNA analysis of significant WGCNA modules

A two-tailed Fisher's exact test was used to test our hypothesis that non-preserved modules were more

likely to contain GWAS identified genes than preserved modules. The risk loci for PD and AD were from recent GWAS, between which only one GWAS gene was shared (*KAT8*) [24, 78].

We gained further insight into SNPs associated with non-preserved modules, using a similar methodology to Chatterjee et al. [17]. The SCAN database [25] was used to find all SNPs that have been shown to predict the expression of each gene within non-preserved modules. For each non-preserved module, only SNPs that predicted gene expression with Pvalues < 1.0e-4 and frequency > 0.10 within the CEU human samples of European descent were selected.

Previous studies have revealed that differential expression of miRNAs were associated with PD [79] and AD [80]. In addition, SNPs have been identified as disease prognostic markers by association to miRNAs [81]. SNPs we found to be associated with genes from the PD related modules were used to search the MirSNP [26] database in order to find which SNPs were associated with the 83 experimentally confirmed PD related miRNAs in the HMDD v3.0 database [82]. The same process was done for genes within the AD related modules and the 57 experimentally confirmed AD related miRNAs in the HMDD v3.0 database. The MirSNP database identified the SNPs that are present at the 3' untranslated region of miRNA target sites, and so narrowed down the selection of SNPs to those that likely effect known miRNAs associated with the disease.

Comparison of PD and AD results

The processes associated with non-preserved modules in AD and PD were compared to see if any processes were similar between diseases. Hub genes and TFs identified in non-preserved modules were also compared between AD and PD to see if any were shared. In addition, we test our hypothesis that AD and PD share SNPs we identified in non-preserved modules associated with disease related miRNAs in AD and PD respectively.

Abbreviations

PD: Parkinson's disease; AD: Alzheimer's disease; HC: Healthy control; TFs: Transcription factors; ND: Neurodegenerative disease; Aβ: amyloid-β1; CNS: Central nervous system; SN: Substantia nigra; DEGs: Differentially expressed genes; WGCNA: Weighted gene co-expression network analysis; MCI: Mild cognitive impairment; ADAD: AD samples from Alzheimer's dataset; ADHC: HC samples from Alzheimer's dataset; ADMCI: MCI samples from Alzheimer's dataset; PDPD: PD samples from Parkinson's dataset; PDHC: HC

samples from Parkinson's dataset; GO: Gene Ontology; KEGG: Kyoto Encyclopedia of Genes and Genomes**;** BC: Betweenness centrality; MM: Module membership; ENCODE: Encyclopedia of DNA Elements; ChIP: Chromatin immunoprecipitation; ChEA: ChIP enrichment analysis; SNP: Single nucleotide polymorphism; GWAS: Genome Wide Association Studies; SCAN: SNP and Copy number Annotation; miRNA: microRNA; PTEN: Phosphatase and tensin homolog; TRPC: Transient receptor potential canonical; BBB: Blood brain barrier; LATE: Limbic-predominant age-related TDP-43 encephalopathy; GEO: Gene Expression Omnibus; RMA: Robust Multiarray Average; MAD: Median absolute deviation; TOM: Topological overlap matrix.

AUTHOR CONTRIBUTIONS

ACKNOWLEDGMENTS

CONFLICTS OF INTEREST

FUNDING

REFERENCES

1. Cacace R, Sleegers K, Van Broeckhoven C. Molecular genetics of early-onset Alzheimer's disease revisited. Alzheimers Dement. 2016; 12:733–48. https://doi.org/10.1016/j.jalz.2016.01.012 PMID:27016693

2. Alzheimer's Association. 2018 Alzheimer's Disease Facts and Figures. 2018. Available from: https://www.alz.org/

3. Shi L, Baird AL, Westwood S, Hye A, Dobson R, Thambisetty M, Lovestone S. A Decade of Blood Biomarkers for Alzheimer's Disease Research: An Evolving sField, Improving Study Designs, and the

Challenge of Replication. J Alzheimers Dis. 2018; 62:1181–98.
https://doi.org/10.3233/JAD-170531
PMID:29562526

4. Long J, Pan G, Ifeachor E, Belshaw R, Li X. Discovery of Novel Biomarkers for Alzheimer's Disease from Blood. Dis Markers. 2016; 2016:4250480.
https://doi.org/10.1155/2016/4250480
PMID:27418712

5. Li X, Long J, He T, Belshaw R, Scott J. Integrated genomic approaches identify major pathways and upstream regulators in late onset Alzheimer's disease. Sci Rep. 2015; 5:12393.
https://doi.org/10.1038/srep12393
PMID:26202100

6. Parkinson's UK. The prevalence and incidence of Parkinson's in the UK. London; 2017.

7. Marras C, Beck JC, Bower JH, Roberts E, Ritz B, Ross GW, Abbott RD, Savica R, Van Den Eeden SK, Willis AW, Tanner CM; Parkinson's Foundation P4 Group. Prevalence of Parkinson's disease across North America. NPJ Parkinsons Dis. 2018; 4:21.
https://doi.org/10.1038/s41531-018-0058-0
PMID:30003140

8. Kalinderi K, Bostantjopoulou S, Fidani L. The genetic background of Parkinson's disease: current progress and future prospects. Acta Neurol Scand. 2016; 134:314–26.
https://doi.org/10.1111/ane.12563
PMID:26869347

9. Xie A, Gao J, Xu L, Meng D. Shared mechanisms of neurodegeneration in Alzheimer's disease and Parkinson's disease. Biomed Res Int. 2014; 2014:648740.
https://doi.org/10.1155/2014/648740
PMID:24900975

10. Anang JB, Nomura T, Romenets SR, Nakashima K, Gagnon JF, Postuma RB. Dementia Predictors in Parkinson Disease: A Validation Study. J Parkinsons Dis. 2017; 7:159–62.
https://doi.org/10.3233/JPD-160925
PMID:27911340

11. Kelly J, Moyeed R, Carroll C, Albani D, Li X. Gene expression meta-analysis of Parkinson's disease and its relationship with Alzheimer's disease. Mol Brain. 2019; 12:16.
https://doi.org/10.1186/s13041-019-0436-5
PMID:30819229

12. Kaźmierczak A, Czapski GA, Adamczyk A, Gajkowska B, Strosznajder JB. A novel mechanism of non-Aβ component of Alzheimer's disease amyloid (NAC) neurotoxicity. Interplay between p53 protein and

cyclin-dependent kinase 5 (Cdk5). Neurochem Int. 2011; 58:206–14.
https://doi.org/10.1016/j.neuint.2010.11.018
PMID:21130128

13. Kwon OD. Is There Any Relationship between Apolipoprotein E Polymorphism and Idiopathic Parkinson's Disease? J Alzheimer's Dis Park. 2017; 7:292.
https://doi.org/10.4172/2161-0460.1000296

14. Miller JA, Oldham MC, Geschwind DH. A systems level analysis of transcriptional changes in Alzheimer's disease and normal aging. J Neurosci. 2008; 28:1410–20.
https://doi.org/10.1523/JNEUROSCI.4098-07.2008
PMID:18256261

15. Langfelder P, Horvath S. WGCNA: an R package for weighted correlation network analysis. BMC Bioinformatics. 2008; 9:559.
https://doi.org/10.1186/1471-2105-9-559
PMID:19114008

16. Lunnon K, Ibrahim Z, Proitsi P, Lourdusamy A, Newhouse S, Sattlecker M, Furney S, Saleem M, Soininen H, Kłoszewska I, Mecocci P, Tsolaki M, Vellas B, et al, and AddNeuroMed Consortium. Mitochondrial dysfunction and immune activation are detectable in early Alzheimer's disease blood. J Alzheimers Dis. 2012; 30:685–710.
https://doi.org/10.3233/JAD-2012-111592
PMID:22466004

17. Chatterjee P, Roy D, Bhattacharyya M, Bandyopadhyay S. Biological networks in Parkinson's disease: an insight into the epigenetic mechanisms associated with this disease. BMC Genomics. 2017; 18:721.
https://doi.org/10.1186/s12864-017-4098-3
PMID:28899360

18. Ritchie SC, Watts S, Fearnley LG, Holt KE, Abraham G, Inouye M. A Scalable Permutation Approach Reveals Replication and Preservation Patterns of Network Modules in Large Datasets. Cell Syst. 2016; 3:71–82.
https://doi.org/10.1016/j.cels.2016.06.012
PMID:27467248

19. Chen EY, Tan CM, Kou Y, Duan Q, Wang Z, Meirelles GV, Clark NR, Ma'ayan A. Enrichr: interactive and collaborative HTML5 gene list enrichment analysis tool. BMC Bioinformatics. 2013; 14:128.
https://doi.org/10.1186/1471-2105-14-128
PMID:23586463

20. Kuleshov MV, Jones MR, Rouillard AD, Fernandez NF, Duan Q, Wang Z, Koplev S, Jenkins SL, Jagodnik KM, Lachmann A, McDermott MG, Monteiro CD, Gundersen GW, Ma'ayan A. Enrichr: a comprehensive gene set enrichment analysis web server 2016 update. Nucleic Acids Res. 2016; 44:W90-7.

https://doi.org/10.1093/nar/gkw377
PMID:27141961

21. Albert R. Scale-free networks in cell biology. J Cell Sci. 2005; 118:4947–57.
https://doi.org/10.1242/jcs.02714
PMID:16254242

22. Richter-Landsberg C, Leyk J. Inclusion body formation, macroautophagy, and the role of HDAC6 in neurodegeneration. Acta Neuropathol. 2013; 126:793–807.
https://doi.org/10.1007/s00401-013-1158-x
PMID:23912309

23. Bastian M, Heymann S, Jacomy M. Gephi: An open source software for exploring and manipulating networks. International AAAI Conference on Weblogs and Social Media. 2009.

24. Chang D, Nalls MA, Hallgrímsdóttir IB, Hunkapiller J, van der Brug M, Cai F, Kerchner GA, Ayalon G, Bingol B, Sheng M, Hinds D, Behrens TW, Singleton AB, et al, and International Parkinson's Disease Genomics Consortium, and 23andMe Research Team. A meta-analysis of genome-wide association studies identifies 17 new Parkinson's disease risk loci. Nat Genet. 2017; 49:1511–16.
https://doi.org/10.1038/ng.3955
PMID:28892059

25. Gamazon ER, Zhang W, Konkashbaev A, Duan S, Kistner EO, Nicolae DL, Dolan ME, Cox NJ. SCAN: SNP and copy number annotation. Bioinformatics. 2010; 26:259–62.
https://doi.org/10.1093/bioinformatics/btp644
PMID:19933162

26. Liu C, Zhang F, Li T, Lu M, Wang L, Yue W, Zhang D. MirSNP, a database of polymorphisms altering miRNA target sites, identifies miRNA-related SNPs in GWAS SNPs and eQTLs. BMC Genomics. 2012; 13:661.
https://doi.org/10.1186/1471-2164-13-661
PMID:23173617

27. Li X, Wang H, Long J, Pan G, He T, Anichtchik O, Belshaw R, Albani D, Edison P, Green EK, Scott J. Systematic Analysis and Biomarker Study for Alzheimer's Disease. Sci Rep. 2018; 8:17394.
https://doi.org/10.1038/s41598-018-35789-3
PMID:30478411

28. Pinho R, Guedes LC, Soreq L, Lobo PP, Mestre T, Coelho M, Rosa MM, Gonçalves N, Wales P, Mendes T, Gerhardt E, Fahlbusch C, Bonifati V, et al. Gene expression differences in peripheral blood of Parkinson's disease patients with distinct progression profiles. PLoS One. 2016; 11:e0157852.
https://doi.org/10.1371/journal.pone.0157852
PMID:27322389

29. Vidal-Martinez G, Yang B, Vargas-Medrano J, Perez RG. Could α-synuclein modulation of insulin and dopamine identify a novel link between parkinson's disease and diabetes as well as potential therapies? Front Mol Neurosci. 2018; 11:465.
https://doi.org/10.3389/fnmol.2018.00465
PMID:30622456

30. Hogg E, Athreya K, Basile C, Tan EE, Kaminski J, Tagliati M. High prevalence of undiagnosed insulin resistance in non-diabetic subjects with Parkinson's disease. J Parkinsons Dis. 2018; 8:259–65.
https://doi.org/10.3233/JPD-181305
PMID:29614702

31. Simões-Pires C, Zwick V, Nurisso A, Schenker E, Carrupt PA, Cuendet M. HDAC6 as a target for neurodegenerative diseases: what makes it different from the other HDACs? Mol Neurodegener. 2013; 8:7.
https://doi.org/10.1186/1750-1326-8-7
PMID:23356410

32. Qu X, Huang C, Qu H, Jia B, Cui Q, Sun C, Chu Y. Histone deacetylase 6 promotes insulin resistance via deacetylating phosphatase and tensin homolog (PTEN) in ovarian OVCAR-3 cells. Int J Clin Exp Pathol. 2016; 9:7105–13.

33. Sekar S, Taghibiglou C. Elevated nuclear phosphatase and tensin homolog (PTEN) and altered insulin signaling in substantia nigral region of patients with Parkinson's disease. Neurosci Lett. 2018; 666:139–43.
https://doi.org/10.1016/j.neulet.2017.12.049
PMID:29288045

34. Shirakawa J, Fernandez M, Takatani T, El Ouaamari A, Jungtrakoon P, Okawa ER, Zhang W, Yi P, Doria A, Kulkarni RN. Insulin signaling regulates the FoxM1/PLK1/CENP-A pathway to promote adaptive pancreatic β-cell proliferation. Cell Metab. 2017; 25:868–882.e5.
https://doi.org/10.1016/j.cmet.2017.02.004
PMID:28286049

35. Lehtonen Š, Sonninen TM, Wojciechowski S, Goldsteins G, Koistinaho J. Dysfunction of cellular proteostasis in Parkinson's disease. Front Neurosci. 2019; 13:457.
https://doi.org/10.3389/fnins.2019.00457
PMID:31133790

36. Santiago JA, Potashkin JA. Blood transcriptomic meta-analysis identifies dysregulation of hemoglobin and iron metabolism in Parkinson' disease. Front Aging Neurosci. 2017; 9:73.
https://doi.org/10.3389/fnagi.2017.00073
PMID:28424608

37. Diner I, Hales CM, Bishof I, Rabenold L, Duong DM, Yi H, Laur O, Gearing M, Troncoso J, Thambisetty M, Lah JJ, Levey AI, Seyfried NT. Aggregation properties of the small nuclear ribonucleoprotein U1-70K in Alzheimer
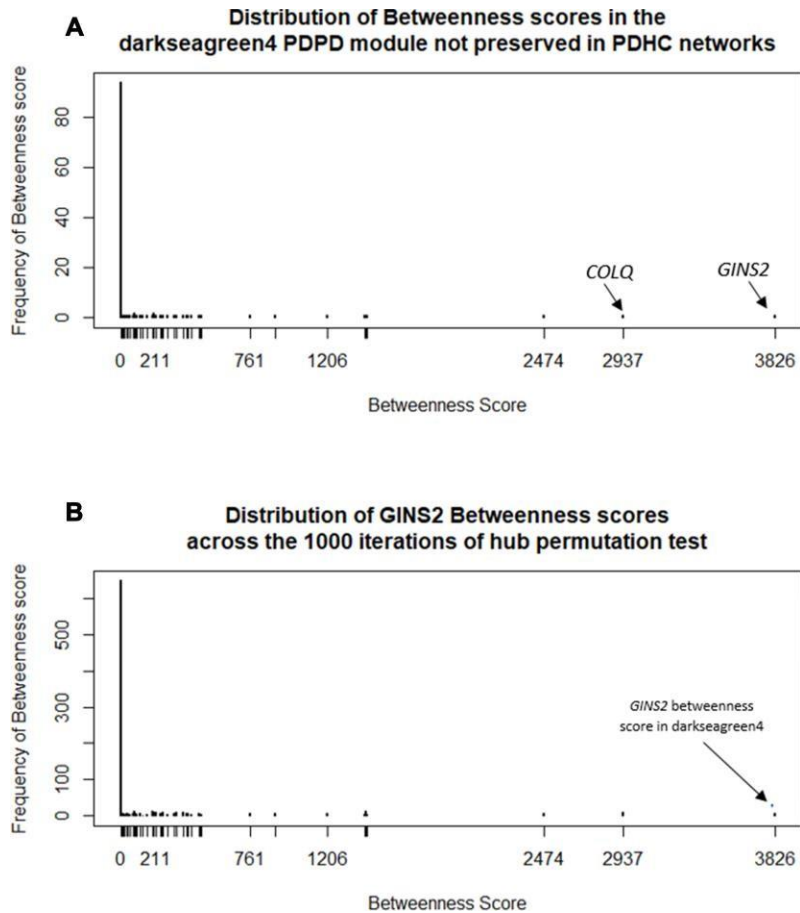
disease. J Biol Chem. 2014; 289:35296–313.
https://doi.org/10.1074/jbc.M114.562959
PMID:25355317

38. Zhang X, Gao F, Wang D, Li C, Fu Y, He W, Zhang J. Tau pathology in Parkinson's disease. Front Neurol. 2018; 9:809.
https://doi.org/10.3389/fneur.2018.00809
PMID:30333786

39. Liu X, Chen J, Guan T, Yao H, Zhang W, Guan Z, Wang Y. miRNAs and target genes in the blood as biomarkers for the early diagnosis of Parkinson's disease. BMC Syst Biol. 2019; 13:10.
https://doi.org/10.1186/s12918-019-0680-4
PMID:30665415

40. Wan Z, Mah D, Simtchouk S, Kluftinger A, Little JP. Role of amyloid β in the induction of lipolysis and secretion of adipokines from human adipose tissue. Adipocyte. 2014; 4:212–16.
https://doi.org/10.4161/21623945.2014.985020
PMID:26257989

41. Ferreira LS, Fernandes CS, Vieira MN, De Felice FG. Insulin Resistance in Alzheimer's Disease. Front Neurosci. 2018; 12:830.
https://doi.org/10.3389/fnins.2018.00830
PMID:30542257

42. Imaizumi T, Ando M, Nakatochi M, Yasuda Y, Honda H, Kuwatsuka Y, Kato S, Kondo T, Iwata M, Nakashima T, Yasui H, Takamatsu H, Okajima H, et al. Effect of dietary energy and polymorphisms in BRAP and GHRL on obesity and metabolic traits. Obes Res Clin Pract. 2018 (Suppl 2); 12:39–48.
https://doi.org/10.1016/j.orcp.2016.05.004
PMID:27245511

43. Albers MW, Gilmore GC, Kaye J, Murphy C, Wingfield A, Bennett DA, Boxer AL, Buchman AS, Cruickshanks KJ, Devanand DP, Duffy CJ, Gall CM, Gates GA, et al. At the interface of sensory and motor dysfunctions and Alzheimer's disease. Alzheimers Dement. 2015; 11:70–98.
https://doi.org/10.1016/j.jalz.2014.04.514
PMID:25022540

44. Murphy C. Olfactory and other sensory impairments in Alzheimer disease. Nat Rev Neurol. 2019; 15:11–24.
https://doi.org/10.1038/s41582-018-0097-5
PMID:30532084

45. Malnic B, Godfrey PA, Buck LB. The human olfactory receptor gene family. Proc Natl Acad Sci USA. 2004; 101:2584–89.
https://doi.org/10.1073/pnas.0307882100
PMID:14983052

46. Casadei E, Tacchi L, Lickwar CR, Espenschied ST, Davison JM, Muñoz P, Rawls JF, Salinas I. Commensal Bacteria Regulate Gene Expression and Differentiation in Vertebrate Olfactory Systems Through Transcription Factor REST. Chem Senses. 2019; 44:615–30.
https://doi.org/10.1093/chemse/bjz050
PMID:31403159

47. Seyfried NT, Dammer EB, Swarup V, Nandakumar D, Duong DM, Yin L, Deng Q, Nguyen T, Hales CM, Wingo T, Glass J, Gearing M, Thambisetty M, et al. A Multi-network Approach Identifies Protein-Specific Co-expression in Asymptomatic and Symptomatic Alzheimer's Disease. Cell Syst. 2017; 4:60–72.e4.
https://doi.org/10.1016/j.cels.2016.11.006
PMID:27989508

48. Poewe W, Seppi K, Tanner CM, Halliday GM, Brundin P, Volkmann J, Schrag AE, Lang AE. Parkinson disease. Nat Rev Dis Primers. 2017; 3:17013.
https://doi.org/10.1038/nrdp.2017.13
PMID:28332488

49. Gray MT, Woulfe JM. Striatal blood-brain barrier permeability in Parkinson's disease. J Cereb Blood Flow Metab. 2015; 35:747–50.
https://doi.org/10.1038/jcbfm.2015.32
PMID:25757748

50. Lue LF, Guerra A, Walker DG. Amyloid Beta and Tau as Alzheimer's Disease Blood Biomarkers: Promise From New Technologies. Neurol Ther. 2017 (Suppl 1); 6:25–36.
https://doi.org/10.1007/s40120-017-0074-8
PMID:28733956

51. Chojdak-Łukasiewicz J, Małodobra-Mazur M, Zimny A, Noga L, Paradowski B. Plasma tau protein and Aβ42 level as markers of cognitive impairment in patients with Parkinson's disease. Adv Clin Exp Med. 2020; 29:115–21.
https://doi.org/10.17219/acem/112058
PMID:31990459

52. Rezai-Zadeh K, Gate D, Szekely CA, Town T. Can peripheral leukocytes be used as Alzheimer's disease biomarkers? Expert Rev Neurother. 2009; 9:1623–33.
https://doi.org/10.1586/ern.09.118
PMID:19903022

53. Li H, Hong G, Lin M, Shi Y, Wang L, Jiang F, Zhang F, Wang Y, Guo Z. Identification of molecular alterations in leukocytes from gene expression profiles of peripheral whole blood of Alzheimer's disease. Sci Rep. 2017; 7:14027.
https://doi.org/10.1038/s41598-017-13700-w
PMID:29070791

54. Cai Z, Qiao PF, Wan CQ, Cai M, Zhou NK, Li Q. Role of Blood-Brain Barrier in Alzheimer's Disease. J Alzheimers Dis. 2018; 63:1223–34.
https://doi.org/10.3233/JAD-180098
PMID:29782323

55. Lin WC, Tsai NW, Huang YC, Cheng KY, Chen HL, Li SH, Kung CT, Su YJ, Lin WM, Chen MH, Chiu TM, Yang IH, Lu CH. Peripheral leukocyte apoptosis in patients with Parkinsonism: correlation with clinical characteristics and neuroimaging findings. BioMed Res Int. 2014; 2014:635923.
https://doi.org/10.1155/2014/635923
PMID:24795890

56. Annesley SJ, Lay ST, De Piazza SW, Sanislav O, Hammersley E, Allan CY, Francione LM, Bui MQ, Chen ZP, Ngoei KR, Tassone F, Kemp BE, Storey E, et al. Immortalized Parkinson's disease lymphocytes have enhanced mitochondrial respiratory activity. Dis Model Mech. 2016; 9:1295–305.
https://doi.org/10.1242/dmm.025684
PMID:27638668

57. Bäckström D, Granåsen G, Domellöf ME, Linder J, Jakobson Mo S, Riklund K, Zetterberg H, Blennow K, Forsgren L. Early predictors of mortality in parkinsonism and Parkinson disease: A population-based study. Neurology. 2018; 91:e2045–56.
https://doi.org/10.1212/WNL.0000000000006576
PMID:30381367

58. Nelson PT, Dickson DW, Trojanowski JQ, Jack CR, Boyle PA, Arfanakis K, Rademakers R, Alafuzoff I, Attems J, Brayne C, Coyle-Gilchrist IT, Chui HC, Fardo DW, et al. Limbic-predominant age-related TDP-43 encephalopathy (LATE): consensus working group report. Brain. 2019; 142:1503–27.
https://doi.org/10.1093/brain/awz099
PMID:31039256

59. Shamir R, Klein C, Amar D, Vollstedt EJ, Bonin M, Usenovic M, Wong YC, Maver A, Poths S, Safer H, Corvol JC, Lesage S, Lavi O, et al. Analysis of blood-based gene expression in idiopathic Parkinson disease. Neurology. 2017; 89:1676–83.
https://doi.org/10.1212/WNL.0000000000004516
PMID:28916538

60. Chai C, Lim KL. Genetic insights into sporadic Parkinson's disease pathogenesis. Curr Genomics. 2013; 14:486–501.
https://doi.org/10.2174/1389202914666131210195808
PMID:24532982

61. Bekris LM, Yu CE, Bird TD, Tsuang DW. Genetics of Alzheimer disease. J Geriatr Psychiatry Neurol. 2010; 23:213–27.
https://doi.org/10.1177/0891988710383571
PMID:21045163

62. Allen JD, Xie Y, Chen M, Girard L, Xiao G. Comparing statistical methods for constructing large scale gene networks. PLoS One. 2012; 7:e29348.
https://doi.org/10.1371/journal.pone.0029348
PMID:22272232

63. Gautier L, Cope L, Bolstad BM, Irizarry RA. affy—analysis of Affymetrix GeneChip data at the probe level. Bioinformatics. 2004; 20:307–15.
https://doi.org/10.1093/bioinformatics/btg405
PMID:14960456

64. Buckberry S, Bent SJ, Bianco-Miotto T, Roberts CT, Massi R. massiR: a method for predicting the sex of samples in gene expression microarray datasets. Bioinformatics. 2014; 30:2084–85.
https://doi.org/10.1093/bioinformatics/btu161
PMID:24659105

65. Leek JT, Johnson WE, Parker HS, Jaffe AE, Storey JD, Zhang Y. sva: Surrogate Variable Analysis. 2019.

66. Wang X, Lin Y, Song C, Sibille E, Tseng GC. Detecting disease-associated genes with confounding variable adjustment and the impact on genomic meta-analysis: with application to major depressive disorder. BMC Bioinformatics. 2012; 13:52.
https://doi.org/10.1186/1471-2105-13-52
PMID:22458711

67. Sood S, Gallagher IJ, Lunnon K, Rullman E, Keohane A, Crossland H, Phillips BE, Cederholm T, Jensen T, van Loon LJ, Lannfelt L, Kraus WE, Atherton PJ, et al. A novel multi-tissue RNA diagnostic of healthy ageing relates to cognitive health status. Genome Biol. 2015; 16:185.
https://doi.org/10.1186/s13059-015-0750-x
PMID:26343147

68. Taminau J, Meganck S, Lazar C, Steenhoff D, Coletta A, Molter C, Duque R, de Schaetzen V, Weiss Solís DY, Bersini H, Nowé A. Unlocking the potential of publicly available microarray data using inSilicoDb and inSilicoMerging R/Bioconductor packages. BMC Bioinformatics. 2012; 13:335.
https://doi.org/10.1186/1471-2105-13-335
PMID:23259851

69. Langfelder P, Zhang B, Horvath S. Defining clusters from a hierarchical cluster tree: the Dynamic Tree Cut package for R. Bioinformatics. 2008; 24:719–20.
https://doi.org/10.1093/bioinformatics/btm563
PMID:18024473

70. Botía JA, Vandrovcova J, Forabosco P, Guelfi S, D'Sa K, Hardy J, Lewis CM, Ryten M, Weale ME, and United Kingdom Brain Expression Consortium. An additional k-means clustering step improves the biological features of WGCNA gene co-expression networks. BMC Syst Biol. 2017; 11:47.
https://doi.org/10.1186/s12918-017-0420-6
PMID:28403906

71. R Core Team. R: A language and environment for statistical computing. Vienna, Austria: R Foundation for Statistical Computing; 2017.

72. Yuan L, Chen L, Qian K, Qian G, Wu CL, Wang X, Xiao Y. Co-expression network analysis identified six hub genes in association with progression and prognosis in human clear cell renal cell carcinoma (ccRCC). Genom Data. 2017; 14:132–140.
https://doi.org/10.1016/j.gdata.2017.10.006
PMID:29159069

73. Brandes U. A faster algorithm for betweenness centrality. J Math Sociol. 2001; 25:163–77.
https://doi.org/10.1080/0022250X.2001.9990249

74. Newman MJ. A measure of betweenness centrality based on random walks. Soc Networks. 2005; 27:39–54.
https://doi.org/10.1016/j.socnet.2004.11.009

75. Kleinberg JM. Authoritative sources in a hyperlinked environment. J Assoc Comput Mach. 1999; 46:604–32.
https://doi.org/10.1145/324133.324140

76. Brin S, Page L. The anatomy of a large-scale hypertextual Web search engine. Comput Netw ISDN Syst. 1998; 30:107–17.
https://doi.org/10.1016/S0169-7552(98)00110-X

77. Csardi G, Nepusz T. The igraph software package for complex network research. Inter Journal. 2006; Complex Sy: 1695.

78. Jansen IE, Savage JE, Watanabe K, Bryois J, Williams DM, Steinberg S, Sealock J, Karlsson IK, Hägg S, Athanasiu L, Voyle N, Proitsi P, Witoelar A, et al. Genome-wide meta-analysis identifies new loci and functional pathways influencing Alzheimer's disease risk. Nat Genet. 2019; 51:404–13.
https://doi.org/10.1038/s41588-018-0311-9
PMID:30617256

79. Martins M, Rosa A, Guedes LC, Fonseca BV, Gotovac K, Violante S, Mestre T, Coelho M, Rosa MM, Martin ER, Vance JM, Outeiro TF, Wang L, et al. Convergence of miRNA expression profiling, α-synuclein interacton and GWAS in Parkinson's disease. PLoS One. 2011; 6:e25443.
https://doi.org/10.1371/journal.pone.0025443
PMID:22003392

80. Zovoilis A, Agbemenyah HY, Agis-Balboa RC, Stilling RM, Edbauer D, Rao P, Farinelli L, Delalle I, Schmitt A, Falkai P, Bahari-Javan S, Burkhardt S, Sananbenesi F, Fischer A. microRNA-34c is a novel target to treat dementias. EMBO J. 2011; 30:4299–308.
https://doi.org/10.1038/emboj.2011.327
PMID:21946562

81. Guo Z, Wang H, Li Y, Li B, Li C, Ding C. A microRNA-related single nucleotide polymorphism of the *XPO5* gene is associated with survival of small cell lung cancer patients. Biomed Rep. 2013; 1:545–48.
https://doi.org/10.3892/br.2013.92
PMID:24648983

82. Huang Z, Shi J, Gao Y, Cui C, Zhang S, Li J, Zhou Y, Cui Q. HMDD v3.0: a database for experimentally supported human microRNA-disease associations. Nucleic Acids Res. 2019; 47:D1013–D1017.
https://doi.org/10.1093/nar/gky1010
PMID:30364956

Supplementary Figure 1. The probe variation plot used to determine which genes to use in massiR R package [53]. A threshold of 4 was selected as it encompassed the genes with the highest variation and ignores genes with low variation that may be useful in classifying samples.

A

Distribution of Betweenness scores in the darkseagreen4 PDPD module not preserved in PDHC networks

B

Distribution of GINS2 Betweenness scores across the 1000 iterations of hub permutation test

Supplementary Figure 2. (**A**) The distribution of betweenness scores for each gene in the darkseagreen4 module. Many genes have a betweenness score of 0 indicating they do not act as hubs in regard to betweenness in this module. After the hub permutation test, one gene was found to be significant (GINS2, Pvalue = 0.005). (**B**) The distribution of betweenness scores for GINS2 over the 1000 iterations of the hub permutation test. The betweenness score of GINS2 in the original darkseagreen4 module network is highlighted.

Supplementary Tables

Supplementary Table 1. Information on number of samples, sex and age of samples in datasets.

GEO Dataset		No. sample	Sex (male/female)	Mean Age (±SD)
GSE99039	PD	204	97/107	NA
	HC	230	150/80	NA
	All	434	247/187	NA
GSE63060 +	AD	245	166/79	76.5 (± 6.6)
GSE63061	MCI	142	79/66	74.9(± 6.3)
	HC	182	110/72	73.6 (± 6.3)
	All	569	352/217	75.2 (±6.5)

Please browse Full Text version to see the data of Supplementary Table 2.

Supplementary Table 2. Excel table of differentially expressed genes found in the PD dataset.

Supplementary Table 3. Excel table of significant hubs found in non-preserved modules between PD and healthy controls.

Module	Gene	Hub detection method	Score	P-value
PD modules not preserved in HC				
	GINS2	Betweenness	3826	0.005
Darkseagreen4	S1PR5	Kleinberg's centrality; PageRank; MM	0.30751; 0.02637; 0.90234	0.006; 0.006; 0.007
	AGBL2	Closeness	10.00256	0.007
	NKG7	PageRank	0.02512	0.007
	SNRNP70	PageRank; Kleinberg's centrality	0.02359; 0.27933	0.003; 0.007
Navajowhite2	POPDC2	Closeness	18.03573	0.008
	CHKB	Kleinberg's centrality	0.28034	0.009
	MIR142	MM	0.85297	0.009
	TYSND1	PageRank; MM; Kleinberg's centrality	0.00978; 0.84787; 0.17499	0.002; 0.002; 0.008
	C17orf97	Closeness	4.4882	0.002
	HDAC6	Kleinberg's centrality; MM; PageRank	0.17867; 0.83636; 0.00958	0.003; 0.006; 0.007
Salmon	FAM114A1	Betweenness	12901	0.004
	ZNF804A	Betweenness; Closeness	12956; 4.27567	0.005; 0.007
	ABCD1	PageRank; MM	0.00904; 0.83955	0.006; 0.006
	ZNF526	PageRank	0.00908	0.006
	TMEM147-AS1	Betweenness	12566	0.008
	RENBP	PageRank	0.00823	0.009
HC modules not preserved in PD				
Purple	FAM110C	Closeness;	0.72585; 33683	0.000; 0.002

TXLNGY	Betweenness Betweenness	40661	0
PAK4	Kleinberg's centrality; Pagerank; MM	0.12262; 0.00467; 0.83401	0.001; 0.002; 0.003
GIGYF1	Kleinberg's centrality; PageRank; MM	0.12332; 0.00473; 0.85428	0.002; 0.002; 0.002
WDTC1	Kleinberg's centrality; MM; PageRank	0.11337; 0.82836; 0.00441	0.002; 0.004; 0.008
NEB	Closeness; Betweenness	0.70015; 21395	0.003; 0.004
SH3BGR	Closeness; Betweenness	0.63727; 19636	0.004; 0.005
FCGBP	Betweenness	16988	0.005
INO80B	PageRank; Kleinberg's centrality; MM	0.00417; 0.10391; 0.82766	0.005; 0.007; 0.007
ZNF582-AS1	Closeness; Betweenness	0.59408; 0.06978	0.006; 0.008
PLA2G4C	Betweenness	20491	0.007
TBC1D25	PageRank; MM	0.00401; 0.81547	0.007; 0.007
MFSD12	Kleinberg's centrality; PageRank; MM	0.10808; 0.00411; 0.80996	0.007; 0.009; 0.009
MCM2	Closeness	0.57973	0.008
SPATA6	Closeness	0.65087	0.009
RPS6KA4	MM	0.80597	0.009
FIZ1	MM	0.81009	0.009

Please browse Full Text version to see the data of Supplementary Table 4.

Supplementary Table 4. Excel table of significant hubs found in non-preserved modules between AD, MCI and healthy controls.

Supplementary Table 5. Excel file containing the significant TFs (Pvalue < 0.01) associated with each non-preserved module between PD and healthy control networks found using Enrichr (ENCODE and ChEA Consensus TFs from ChIP-X).

Module colour	Significant TFs	P-value	Gene overlap
PD modules not preserved in HC			
Darkseagreen4	FOXM1	4.004E-08	9/95
	E2F4	8.131E-08	21/710
Navajowhite2	RUNX1	0.008305	18/1294
Salmon	FOXM1	0.006578	6/95
HC modules not preserved in PD			
	SIX5	0.0001626	55/1094
	ZBTB7A	0.0002814	94/2184
	SRF	0.0008434	20/299
Purple	CREB1	0.001402	64/1444
	NFYB	0.004818	138/3715
	PBX3	0.007364	54/1269

Supplementary Table 6. Excel file containing the significant TFs (Pvalue < 0.01) associated with each non-preserved module between AD, MCI and healthy control networks found using Enrichr (ENCODE and ChEA Consensus TFs from ChIP-X).

Module colour	Significant TFs	P-value	Gene overlap
AD modules not preserved in HC and MCI			
Blue	SUZ12	3.36E-10	150/1684
	EZH2	0.0004579	26/237
MCI modules not preserved in AD and HC			
Sienna3	SUZ12	8.24E-10	115/1684
HC modules not preserved in AD and MCI			
Darkolivegreen	SUZ12	0.00392	68/1684
	REST	0.009205	20/383
	IRF3	0.000002884	24/663
	SP2	0.000006359	30/994
	NFYB	0.0000105	74/3715
	GABPA	0.00001689	48/2082
	BRCA1	0.0003388	61/3218
	CTCF	0.0003775	39/1790
Darkorange2	NFYA	0.0004409	46/2250
	PBX3	0.0005193	30/1269
	SIX5	0.00115	26/1094
	SMC3	0.003293	26/1181
	NR2C2	0.004466	11/350
	FOS	0.006121	16/637
	CREB1	0.007005	29/1444
Skyblue	RCOR1	0.002542	15/702
	BCLAF1	0.006338	16/851
HC modules not preserved in MCI			
Red	SUZ12	1.21E-09	107/1684
	EZH2	0.0001041	21/237

Supplementary Table 7. Excel file containing the SNPs associated with PD SNPs in bold are shared between PD and AD.

Chromosome	SNPs	Associated PD related miRNAs	Modules with SNP associated gene	Genes
1	rs12140193	hsa-miR-495	PD darkseagreen4	METTL13
	rs1138729	hsa-miR-495	PD salmon	RRM2
	rs12603	hsa-miR-543	HC purple	EPB41L5
2	rs2058703	hsa-miR-1283	HC purple; PD salmon	BCL11A
	rs4852735	hsa-miR-4271	PD navajowhite2	TEX261
	rs707718	hsa-miR-543	HC purple	CYP26B1
3	**rs1135750**	hsa-miR-147a	PD navajowhite2	IQCB1
	rs11551405	hsa-miR-203	HC purple	DCP1A
4	rs3805317	hsa-miR-203	HC purple	CLGN
5	rs2561659	hsa-miR-543	HC purple	AHRR
6	**rs12528857**	hsa-miR-203	HC purple; PD darkseagreen4; PD salmon; PD navajowhite2	TDRD6
	rs1966	hsa-miR-543	HC purple; PD darkseagreen4	PSORS1C1
7	**rs1044718**	hsa-miR-147a	HC purple; PD darkseagreen4; PD salmon	PARP12
8	**rs2929969**	hsa-miR-133b; hsa-miR-203	PD darkseagreen4	WISP1
9	rs7047770	hsa-miR-133b	HC purple; PD navajowhite2	C9orf139
	rs818055	hsa-miR-147a	HC purple; PD navajowhite2	LAMC3
10	rs1042192	hsa-miR-376b	HC purple	CYP2C18
	rs10832733	hsa-miR-543	HC purple	PIK3C2A
11	rs2512676	hsa-miR-147a	PD darkseagreen4; PD salmon	DLG2
	rs7126647	hsa-miR-543	PD navajowhite2	MRGPRX2
	rs9444	hsa-miR-495	HC purple	RNF169
14	**rs1054195**	hsa-miR-543	PD navajowhite2	CLMN
16	rs1568391	hsa-miR-495	PD darkseagreen4	IRF8
17	**rs3744711**	hsa-miR-203	HC purple; PD salmon	DHX33
18	rs1790974	hsa-miR-203	HC purple	DOK6
	rs3745067	hsa-miR-4271	HC purple; PD darkseagreen4; PD salmon	ONECUT2
19	rs36621	hsa-miR-376b	PD navajowhite2	TSEN34
20	rs1060347	hsa-miR-134	HC purple	PCMTD2
22	rs712979	hsa-miR-203	HC purple	C22orf39

Supplementary Table 8. Excel file containing the SNPs associated with AD SNPs in bold are shared between AD and PD.

Chromosome	SNPs	Associated PD related miRNAs	Modules with SNP associated gene	Genes
1	rs6660019	hsa-miR-433	AD blue; HC darkolivegreen; MCI sienna3	SASS6
2	**rs12603**	hsa-miR-543	HC darkorange2	EPB41L5
	rs707718	hsa-miR-543	AD blue; HC darkolivegreen; HC red; MCI sienna3	CYP26B1
	rs1135750	hsa-miR-147a	HC skyblue	IQCB1
3	**rs11551405**	hsa-miR-203	AD blue; HC darkorange2; HC red	DCP1A
	rs340833	hsa-miR-433	HC skyblue	IL5RA
	rs6792607	hsa-miR-153	HC skyblue	EIF5A2
4	**rs3805317**	hsa-miR-203	AD blue; HC red; MCI sienna3	CLGN
	rs8336	hsa-miR-203	AD blue	SMARCAD1
	rs10864	hsa-miR-433	AD blue; HC red; MCI sienna3	BCKDHB
6	**rs12528857**	hsa-miR-203	AD blue; HC darkorange2; HC red; MCI sienna3	TDRD6
	rs1966	hsa-miR-543	AD blue; HC red; MCI sienna3	PSORS1C1
	rs4709266	hsa-miR-433	AD blue; HC red; MCI sienna3	TAGAP
7	**rs1044718**	hsa-miR-147a	HC red	PARP12
	rs1042992	hsa-miR-495	HC darkorange2	BNIP3L
8	**rs2929969**	hsa-miR-133b; hsa-miR-203	AD blue	WISP1
	rs732338	hsa-miR-134	AD blue; HC red; MCI sienna3	LZTS1
10	rs7071789	hsa-miR-495	HC darkolivegreen	TRUB1
11	**rs10832733**	hsa-miR-543	HC darkorange2	PIK3C2A
14	**rs1054195**	hsa-miR-543	AD blue; MCI sienna3	CLMN
16	rs7294	hsa-miR-147a	HC darkolivegreen	VKORC1
17	**rs3744711**	hsa-miR-203	HC darkorange2; HC skyblue	DHX33
18	rs1046699	hsa-miR-433	AD blue; HC red; MCI sienna3	C18orf54
	rs608823	hsa-miR-433	AD blue; HC red; MCI sienna3	ONECUT2
21	rs243609	hsa-miR-543	AD blue; HC red; MCI sienna3	C21orf91
22	rs137124	hsa-miR-134	AD blue	CYB5R3
	rs17032	hsa-miR-495	HC darkolivegreen	SUN2